Structure and transformation of the metastable boron- and oxygen-related defect center in crystalline silicon

Jan Schmidt* and Karsten Bothe
Institut für Solarenergieforschung Hameln/Emmerthal (ISFH), Am Ohrberg 1, D-31860 Emmerthal, Germany
(Received 2 September 2003; published 22 January 2004)

We analyze the core structure of the carrier-lifetime-reducing boron- and oxygen-related metastable defect center in crystalline silicon by measuring the correlation of the defect concentration with the boron and the oxygen contents on a large number of different silicon materials. The experimental results indicate that the defect is composed of one substitutional boron and two interstitial oxygen atoms. Formation and annihilation of the metastable boron-oxygen complex are found to be thermally activated processes, characterized by two strongly differing activation energies. Measurements of the defect generation rate as a function of light intensity show that the defect generation rate increases proportionally with light intensity below 1 mW/cm^2 and saturates at higher intensities. All experimental results can be consistently explained using a defect reaction model based on fast-diffusing oxygen dimers (O_{2i}), which are captured by substitutional boron (B_s) to form a metastable B_s-O_{2i} complex. Based on this model, new strategies for an effective reduction of the light degradation of solar cells made on oxygen-rich silicon materials are derived. The model also explains why no lifetime degradation is observed in aluminum-, gallium-, and indium-doped oxygen-rich silicon.

DOI: 10.1103/PhysRevB.69.024107 PACS number(s): 61.72.Yx, 61.72.Ji, 61.72.Cc

I. INTRODUCTION

Solar cells made on B-doped Czochralski silicon (Cz-Si) degrade under illumination by up to 10% (relative) in efficiency. Although already known since 1973,[1] a conclusive explanation of this material-related effect is still to be found. In retrospect, a central problem of the early studies on this effect might have been the distinction between the fundamental effect (which is now known to be not only restricted to solar-grade Cz-Si, but is present in *all* oxygen-rich boron-doped silicon materials, even if they are of highest purity) and metal-impurity-related degradation effects such as the dissociation of the iron-boron pair.[2] This might have been one of the reasons why it was not until 1997 that the first metal-impurity-free defect reaction model capable of explaining the fundamental degradation effect as well as the characteristic recovery behavior during low-temperature annealing was proposed.[3] In this model, a lifetime-reducing recombination center made up of one interstitial boron (B_i) and one interstitial oxygen (O_i) atom is created under illumination (B_iO_i). Large concentrations of oxygen are virtually unavoidable in Cz-Si due to the partial dissolution of the silica crucible during the growth process. Interestingly, it was found that Ga-doped and P-doped Cz silicon as well as oxygen-lean float-zone (FZ) silicon samples do not present any lifetime degradation effect, which is thus exclusively linked to the *simultaneous* presence of boron and oxygen in the material.[3] According to recent theoretical considerations of Ohshita *et al.*,[4] the B_iO_i pair could only exist in a stable configuration if a substitutional silicon atom would be sited between the boron and the oxygen atom. Glunz *et al.*[5] verified the correlation with boron and oxygen, previously reported by Schmidt *et al.*[3] However, whereas they found an approximately linear increase in the lifetime degradation with boron doping concentration, a strongly superlinear increase with oxygen concentration, approximately to the power of 5, was reported. These results gave rise to the suspicion that the metastable recombination center is probably associated with a defect complex different from the B_iO_i pair. Moreover, it is highly doubtful if any interstitial boron exists in non-particle-irradiated silicon at all. These considerations were further supported by measurements of Schmidt and Cuevas[6] using injection-level-dependent lifetime spectroscopy. They showed that the energy level of the light-induced recombination center is very different from that of the B_iO_i pair and proposed a new core structure consisting of one substitutional boron (B_s) and several oxygen atoms. More recently, Bourgoin *et al.*[7] proposed a possible atomic configuration of the boron-oxygen complex in which the B_s atom is surrounded by three O_i atoms. They also suggested a new degradation mechanism in which electron trapping induces a Jahn-Teller distortion, shifting one of the energy levels of the defect to midgap. However, the proposed mechanism could not be experimentally verified up to now.

In this paper, we present experimental results on the B_s and O_i dependence of the metastable defect concentration, measured on more than 30 different silicon materials. Furthermore, temperature- and intensity-dependent measurements of the defect generation process and a detailed study of the annihilation kinetics are presented. The measurements provide clear experimental evidence of our recently suggested oxygen-dimer model.[8]

II. COMPOSITION OF THE DEFECT

In a recent contribution,[8] we have presented preliminary experimental results on the boron and oxygen dependence of the metastable defect concentration. We have now extended our data base considerably. The effective carrier lifetimes were measured before (τ_0) and after (τ_d) complete light degradation at a well-defined injection level Δn using the quasi-steady-state photoconductance (QSSPC) technique.[9] Surface passivation was realized using plasma-enhanced chemical-

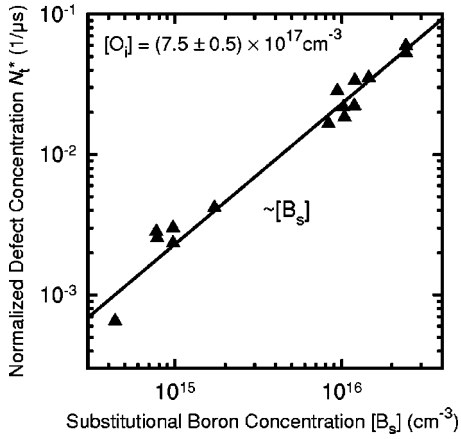

FIG. 1. Measured normalized defect concentration N_t^* as a function of the substitutional boron concentration $[B_s]$ for Cz-Si wafers with similar oxygen concentrations $[O_i]$. The fitted curve shows that N_t^* increases proportionally with $[B_s]$.

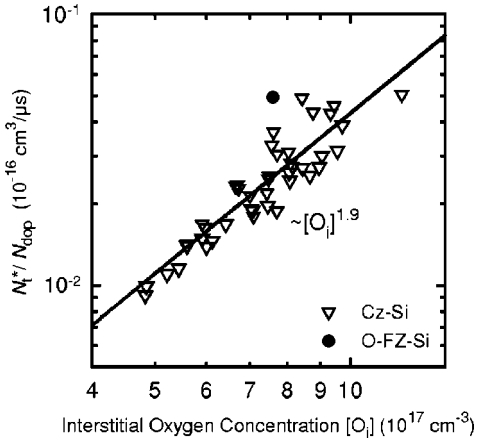

FIG. 2. Measured ratio of the normalized defect concentration N_t^* to the doping concentration N_{dop} as a function of the interstitial oxygen concentration $[O_i]$ for a large number of different Cz-Si samples. Also included is one data point of an oxygen-rich FZ silicon wafer (O-FZ-Si). The solid line is fitted to the measured data and follows a power law $N_t^*/N_{dop} \sim [O_i]^{1.9}$.

vapor-deposited silicon nitride films deposited onto both wafer surfaces at low temperature (400 °C).[10] From the measured τ_0 and τ_d data, the normalized defect concentration $N_t^* \equiv 1/\tau_d - 1/\tau_0$ was calculated.

Figure 1 shows the measured dependence of N_t^* on the substitutional boron concentration $[B_s]$ for various Cz-Si materials with similar levels of oxygen contamination $[O_i] = (7-8)\times 10^{17}$ cm^{-3}. The B_s concentrations equal the doping densities N_{dop} of the wafers and were directly calculated from the wafer resistivities obtained from eddy current and four point probe measurements. All lifetime data were measured at a fixed injection level of $\eta = \Delta n/N_{dop} = 0.1$, which is close to low-level injection, but large enough to avoid any minority-carrier trapping effects.[11] Note that in our previous publications[6,8] we have analyzed the low-level injection lifetimes determined by fitting the complete injection-dependent lifetime curves. The benefit of evaluating the lifetime data at a fixed injection level is that it is not necessary to measure the complete injection level dependence of the carrier lifetime over a broad injection range. As can be seen from Fig. 1, the measured data points show a nearly perfect *proportional* increase of N_t^* with increasing $[B_s]$. Since this finding is in excellent agreement with the results of several previous studies,[5,6,8] the linear dependence of the metastable defect concentration on the boron concentration may now be regarded as firmly established.

A much broader scattering in the data points has been found for the $N_t^*(O_i)$ dependence.[5,8] In our earlier paper,[8] Cz-Si materials with similar boron doping concentrations have been measured, limiting the number of data points considerably. We have now extended our data base including Cz-Si materials with different B_s concentrations and dividing the measured N_t^* values by the corresponding doping concentrations $N_{dop} = [B_s]$. This procedure assumes a proportional dependence of N_t^* on N_{dop},[12] which is experimentally verified in Fig. 1.

In Fig. 2, N_t^*/N_{dop} is plotted versus $[O_i]$. The carrier lifetimes were again measured at a constant injection level of $\eta = 0.1$. The interstitial oxygen concentrations were determined according to DIN 50438-1 using a Bruker Equinox 55 FTIR spectrometer. The solid line in Fig. 2 shows the fit of a power law $N_t^* \sim [O_i]^{\alpha}$, with $\alpha = 1.9$, to the measured data. The *quadratic* increase of the defect concentration with increasing $[O_i]$ is in excellent agreement with our previously published data.[8] The important difference to our recent study is the hugely extended data base, strengthening the foundations for the oxygen-dimer model, which will be discussed in Sec. V. Compared to the $N_t^*(B_s)$ measurements shown in Fig. 1, the scattering of the data points in Fig. 2 is much larger, suggesting an indirect participation of interstitial oxygen in the defect complex. Also included in Fig. 2 is one data point of a boron-doped oxygen-rich FZ-Si wafer (O-FZ-Si), which shows the same lifetime degradation behavior as Cz-Si, supporting that it is exclusively the simultaneous presence of boron and oxygen causing the lifetime degradation and not the crystal growth technique. Moreover, we have investigated silicon wafers grown by the magnetic-field assisted Czochralski method (MCz-Si), having strongly reduced oxygen contents. Including the MCz-Si wafers into Fig. 2 results in a slightly weaker $N_t^*(O_i)$ dependence. These results are discussed in detail in a separate paper.[13]

The quadratic dependence of the defect concentration on $[O_i]$ is a much weaker dependence compared to that found by Glunz *et al.*[5] This discrepancy might, to a certain extent, be due to the different measurement conditions applied in both studies. While our lifetime data were measured at a fixed injection level, the measurements in Ref. 5 were performed at a constant bias light intensity, resulting in different injection levels for samples with varying lifetimes. Moreover, the samples in Ref. 5 were thermally oxidized at high temperature (>1000 °C) to passivate the wafer surfaces. Such a high-temperature treatment might alter the $N_t^*(O_i)$ dependence.

III. DEFECT FORMATION

We have performed measurements of the time-dependent normalized defect concentration $N_t^*(t)$ on a standard 1.1-

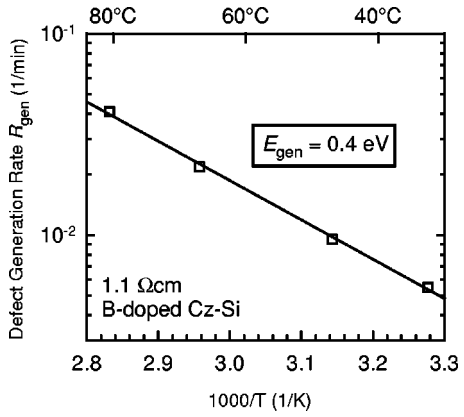

FIG. 3. Arrhenius plot of the defect generation rate R_{gen}. The linear dependence shows that the defect generation is a thermally activated process characterized by an activation energy of $E_{gen} = 0.4$ eV.

Ωcm B-doped Cz-Si material. Between each measurement, the Cz-Si sample was illuminated with a halogen lamp at 10 mW/cm^2 at temperatures ranging from 45 to 100 °C. In this temperature range, defect annihilation can be completely neglected. The defect generation rate $R_{gen}(T)$ was determined by fitting the function

$$N_t^*(t,T) = N_t^*(t \to \infty)[1 - \exp(-R_{gen}(T)t)] \qquad (1)$$

to the measured data. The initial very fast decay of the carrier lifetime, observed during the first few seconds of light soaking, was not analyzed in this study. Figure 3 shows the Arrhenius plot of R_{gen} as a function of inverse temperature $1/T$. The measured linear dependence in Fig. 3 clearly proves that the physical mechanism responsible for the lifetime degradation in boron-doped Cz-Si solar cells is a *thermally activated* process with a relatively low activation energy of $E_{gen} = 0.4$ eV. This finding suggests a diffusion-limited defect formation mechanism.

Figure 4 shows the evolution of $N_t^*(t)$ at different illumination intensities. During light soaking, the 1.5-Ωcm Cz-Si

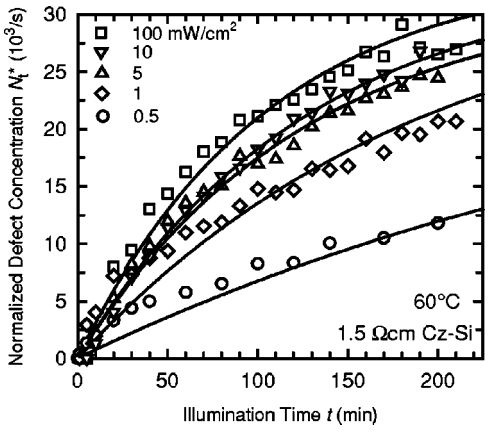

FIG. 4. Evolution of the measured normalized defect concentration $N_t^*(t)$ for a 1.5-Ωcm B-doped Cz-Si sample at different illumination intensities. The sample was kept at a constant temperature of 60 °C during illumination.

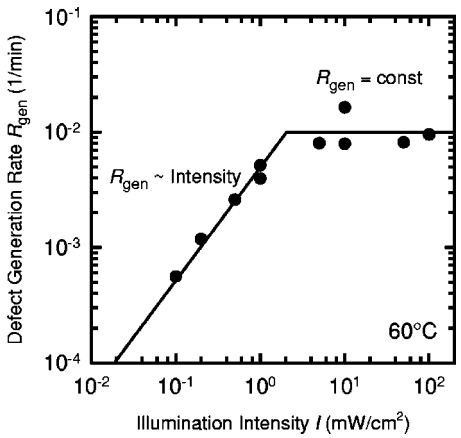

FIG. 5. Measured defect generation rate R_{gen} as a function of illumination intensity I for a 1.5 Ωcm B-doped Cz-Si sample. R_{gen} increases proportionally with I at low light intensities ($I < 1$ mW/cm^2) and saturates at higher intensities.

sample was kept at a fixed temperature of 60 °C. The corresponding fits (solid lines in Fig. 4) give the generation rate R_{gen} as a function of the light intensity I. Figure 5 shows the corresponding $R_{gen}(I)$ dependence. At very low intensities below about 1 mW/cm^2, the increase in R_{gen} is directly proportional to the increase in light intensity. Such a dependence would be expected from a recombination-enhanced defect formation process, requiring a proportional relationship between the defect generation rate R_{gen} and the photogeneration rate G, which equals under steady-state conditions the recombination rate U. At intensities above 1 mW/cm^2, R_{gen} saturates at a value of 10^{-2} 1/min. A very similar behavior has recently been observed by Hashigami *et al.*[14] on Cz-Si solar cells.

IV. DEFECT ANNIHILATION

Rein *et al.* have shown recently that the defect annihilation is a thermally activated process.[15] To determine the activation energy E_{ann} of this process, they performed *in situ* lifetime measurements using a microwave-detected photoconductance decay (MW-PCD) setup with an integrated cryostat. The measurements were carried out in a temperature range from 110 to 150 °C and resulted in an activation energy of $E_{ann} = 1.3$ eV. In a more recent study, we have verified the thermal activation of the annihilation process, but obtained a higher activation energy of 1.8 eV.[8] In contrast to the study of Rein *et al.*,[15] we used the QSSPC method and performed the lifetime measurements at room temperature. Hence, during the measurement of each annihilation curve the samples were alternately annealed in the dark at a controlled temperature between 115 and 145 °C and measured at room temperature. The permanent temperature cycling during the recording of one annihilation curve is a fundamental drawback of this method.

Due to the relatively large measurement error of our previous method, we have developed a new approach for a more accurate determination of E_{ann}. This approach is based on illuminating the samples during annealing and measuring the lifetime saturation value only.

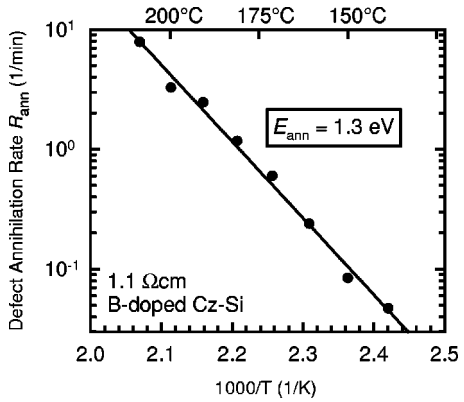

FIG. 6. Arrhenius plot of the defect annihilation rate R_{ann}. The linear dependence shows that the defect annihilation is a thermally activated process characterized by an activation energy of $E_{ann} = 1.3$ eV.

Taking into account that in this experiment annihilation and generation occur simultaneously, the time dependence of N_t^* is determined via the differential equation

$$\frac{dN_t^*(t)}{dt} = R_{gen}[N_{t.max}^* - N_t^*(t)] - R_{ann}N_t^*(t), \qquad (2)$$

where $N_{t.max}^*$ is the maximum defect concentration. Prior to illumination, the sample is annealed in the dark at 200 °C, so that $N_t^*(t=0)=0$ and the solution of Eq. (2) becomes

$$N_t^*(t) = \frac{R_{gen}}{R_{gen}+R_{ann}} N_{t.max}^*[1-\exp(-(R_{gen}+R_{ann})t)]. \qquad (3)$$

The characteristic decay time constant of this process $1/(R_{gen}+R_{ann})$ is much faster compared to the isolated annihilation and generation processes. Hence, after a relatively short period, in our experiments it was always below 1 min, the defect concentration saturates. The defect annihilation rate $R_{ann}(T)$ can now directly be calculated from the saturation value of the normalized defect concentration $N_t^*(t \rightarrow \infty)$, the maximum possible defect concentration $N_{t.max}^*$ and the defect generation rate $R_{gen}(T)$ as known from the measurements shown in Fig. 3:

$$R_{ann} = \left(\frac{N_{t.max}^*}{N_t^*} - 1\right) R_{gen}. \qquad (4)$$

Using this method, we are able to extend the temperature range up to 210 °C. Figure 6 shows the corresponding Arrhenius plot of R_{ann}. The activation energy obtained from the fit to the measured data is $E_{ann} = 1.3$ eV, which is in excellent agreement with the results of the dynamic lifetime measurements.[15]

V. DEFECT MODEL

Assuming the lifetime degradation in boron-doped oxygen-rich silicon is due to an actual defect reaction (and not just due to a change of the defect configuration as proposed in Ref. 7), the dependence of the metastable defect concentration N_t^* on $[B_s]$ and $[O_i]$ (Sec. II) suggests that a reaction between a cluster of oxygen atoms and a boron atom occurs. As substitutional boron is largely immobile in the silicon lattice and interstitial boron exists only in negligible amounts in non-particle-irradiated silicon, we have developed a defect reaction model in which an oxygen cluster is the mobile species in the defect reaction.[8] Small oxygen agglomerates, in particular the oxygen dimer O_{2i}, which is made up of two O_i atoms, can be extremely fast diffusers in silicon.[16,17] The diffusivity of the oxygen dimer in silicon is known to be several orders of magnitude higher than the diffusivity of interstitial atomic oxygen.[18] The fast-diffusing O_{2i} dimers are captured by substitutional boron B_s to form a B_s-O_{2i} complex, which acts as a highly effective recombination center. Due to the fact that the tetrahedral covalent radius of the B atom (0.88 Å) is 25% smaller than that of the Si host atom (1.17 Å),[19] the O_{2i} is preferentially accommodated in the vicinity of a B atom.

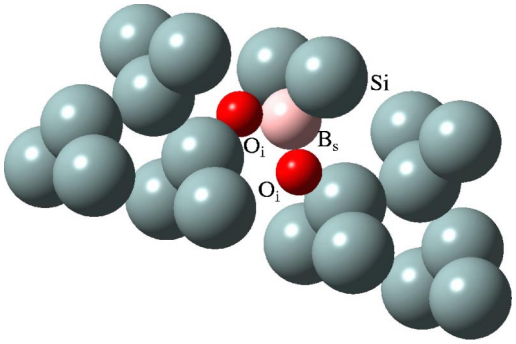

FIG. 7. (Color online) Estimated configuration of the metastable B_s-O_{2i} complex in the silicon host lattice.

As the defect formation process is governed by the diffusion of the oxygen dimer, it is a thermally activated process, which agrees well with our experimental findings presented in Sec. III. Figure 7 shows an estimated configuration of the metastable B-O_2 complex based on theoretical calculations of the stable dimer structure, which is believed to be a 'puckered dimer' structure, where both oxygen atoms sit bond-centered in a kinked Si-O-Si bond.[20] The proposed B-O_2 structure bears a certain similarity to the Al-O_2 complex identified by Gregorkiewicz *et al.*[21] using electron-nuclear double resonance. In their Al-O_2 model,[21] the aluminum atom is shifted from its substitutional position to a tetrahedral interstitial site, creating a vacancy. On the basis of our measurements we cannot rule out that in the boron-oxygen complex, a similar shift of the boron atom might occur during the reaction with the oxygen dimer and a vacancy is created. This would imply that the energy levels of the boron-oxygen complex in the forbidden bandgap would mainly be determined by the interaction of the vacancy with the oxygen atoms. Hence, B_i-V-O_{2i} seems to be another possible structure for the metastable boron-oxygen complex.

There are two possible mechanisms concerning the role of the illumination or, generally speaking, the minority-carrier injection. The minority carriers are in both cases not directly involved in the defect reaction, but their presence triggers the

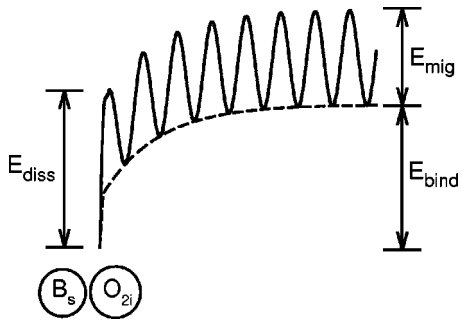

FIG. 8. Energy diagram of the B_s-O_{2i} interaction.

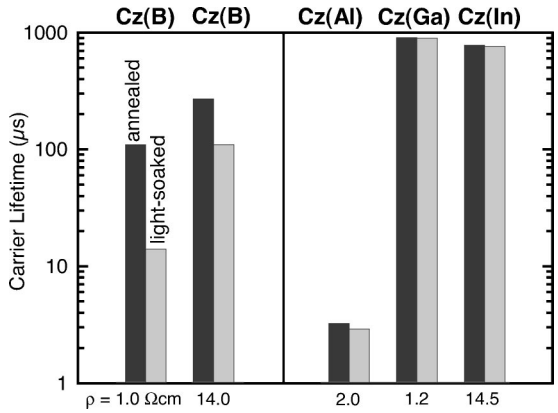

FIG. 9. Effect of light-soaking on the carrier lifetime of Al-, Ga-, and In-doped Cz-Si wafers of different resistivities ρ compared with conventional B-doped Cz-Si. The O_i concentrations of all materials are in the range of $(7-8)\times10^{17}$ cm^{-3}.

reaction by (i) changing the charge state of the O_{2i}, which might lead to an increase in the O_{2i} diffusivity; or (ii) enhancing the O_{2i} diffusivity via a recombination-enhanced diffusion process.[22] Voltage- and temperature-dependent measurements of the dark degradation behavior of Cz-Si solar cells have been performed by the authors to decide which process applies.[23,24] If mechanism (i) would apply, the shift of the threshold voltage above which the degradation occurs should show the same temperature dependence as the Fermi level. However, it turns out that the experimentally observed temperature dependence is much stronger and, hence, mechanism (i) can be excluded.[24] On the other hand, mechanism (ii) would be in good agreement with the experimental results presented in Fig. 5. At low light intensities (<1 mW/cm^2) we find a proportional increase in the defect generation rate R_{gen} with increasing photogeneration rate G. Under steady-state conditions, G equals the recombination rate U. Consequently, our results prove that $R_{gen}\sim U$ at low light intensities, clearly pointing to a recombination-enhanced defect formation process. The observed saturation in R_{gen} for light intensities above 1 mW/cm^2 may be attributed to the relatively low concentration of O_{2i} dimers in the silicon lattice. Process (ii) is also in excellent agreement with our recent finding that the defect generation rate depends only on the total number of minority carriers and is hence also present under equilibrium conditions in the dark at elevated temperatures. Details on this surprising behavior have been published recently.[23]

Figure 8 shows a schematic energy diagram of the interaction of O_{2i} and B_s. The formation and dissociation reaction of the proposed B_s-O_{2i} complex are determined by three characteristic energies: the binding energy E_{bind}, the migration energy of the oxygen dimer E_{mig}, and the dissociation energy of the complex E_{diss}. E_{mig} has been calculated very recently by Lee *et al.*[18] on the basis of density-functional-theoretic total-energy calculations. They found that E_{mig} of the O_{2i} dimer in silicon lies between 0.3 and 1 eV. For comparison, the migration energy of O_i in silicon is as high as 2.5 eV. The migration energy E_{mig} corresponds to the activation energy of the defect generation process as determined in Sec. III: $E_{mig}=E_{gen}=0.4$ eV. This migration energy is much lower than that of O_i in silicon. Hence, we can exclude the direct participation of O_i in the boron-oxygen complex, which is in good agreement with the large scatter in the $N_t^*(O_i)$ data of Fig. 2. However, $E_{mig}=0.4$ eV is consistent with the migration energy range calculated by Lee *et al.*[18] for the oxygen dimer. Using infrared absorption spectroscopy, Åberg *et al.*[25] have determined the activation energy of the diffusivity of the oxygen dimer in the temperature range 350–420 °C. In their study, the 1013-cm^{-1} absorption band was associated with the fast-diffusing oxygen dimer. The experimental data could be reproduced by a model assuming a sequential generation of oxygen clusters, and a migration energy of 1.3 eV was determined for the dimer.[25] However, taking the migration of the oxygen trimer into account, much lower migration energies (<1 eV) were found to be capable of reproducing the experimental data of Åberg *et al.*[18] When comparing these results with the activation energy of the defect formation process investigated in this paper, care has to be taken, because very different temperature ranges are compared. Unfortunately, no experimental data on the agglomeration of oxygen atoms has been published so far in the very low temperature range $\leqslant$100 °C studied in this work.

The second characteristic energy determined from our measurements is the dissociation energy of the defect complex, which corresponds to the activation energy of the defect annihilation process: $E_{diss}=E_{ann}=1.3$ eV. Unfortunately, a direct calculation of E_{bind} from E_{diss} and E_{mig} is not possible. However, because $E_{bind}>E_{diss}-E_{mig}$, we are able to determine a lower bound to the binding energy $E_{bind.low}=E_{diss}-E_{mig}=0.9$ eV.

VI. REDUCING THE LIFETIME DEGRADATION

A. Alternative acceptors (Al, Ga, In)

Figure 9 shows the effect of light-soaking on the carrier lifetime of Al-, Ga-, and In-doped Cz-Si compared with standard B-doped Cz-Si. The carrier lifetimes in Fig. 9 were measured by the MW-PCD technique at a fixed bias light intensity of 30 mW/cm^2. The O_i concentrations of all materials in Fig. 9 are in the range of $(7\text{-}8)\times10^{17}$ cm^{-3}. In contrast to the B-doped Cz-Si materials, no lifetime degradation is observed in Cz-Si doped with Al, Ga, or In. How-

ever, in the case of the Al-doped Cz-Si very low lifetimes of only a few microseconds are measured, which may be attributed to a specific Al-related defect species always present in Al-doped oxygen-rich silicon.[26] We have examined Al-doped Cz-Si materials of different manufacturers and the lifetimes have always been well below the level typical for B-doped Cz-Si. On the other hand, lifetimes in Ga-and In-doped Cz-Si wafers reach values of several hundred microseconds and are perfectly stable under illumination. The exceptionally high electronic quality and perfect stability of Ga-doped Cz-Si has been discussed before.[3,27]

Using the defect reaction model presented in Sec. V, we are able to explain the excellent stability of Al-, Ga-, and In-doped Cz-Si. The key seems to be the tetrahedral radii of the different elements. While the B atom is 25% *smaller* than the Si host atom, the tetrahedral covalent radii of Al, Ga, and In are 8–23 % *greater* compared to that of the Si atom.[19] Hence, there is not enough space available in the vicinity of these three dopant atoms to accommodate the O_{2i} dimer.

According to Fig. 9, Ga- and In-doped Cz-Si are ideally suited materials for the manufacture of stable high-efficiency silicon solar cells. In fact, stable solar cell efficiencies exceeding 20% have already been realized on Ga-doped Cz-Si materials.[28,29] The only drawback of Ga as an alternative dopant element in Cz-Si is the relatively low segregation coefficient, which is two orders of magnitude below that of B in Si. Hence, Ga-doped Cz-Si crystals exhibit a considerably higher variation in resistivity along their growth axis compared to B-doped crystals. Metz *et al.* have investigated the usability of a complete Ga-doped Cz-Si ingot in their high-efficiency obliquely evaporated contact solar cell process and found that the resistivity variations are well tolerable.[28] As the segregation coefficient of In in Si is more than three orders of magnitude below that of B in Si, it is highly likely that the use of In-doped silicon grown by the conventional Cz method would lead to intolerable resistivity variations along the crystal axis. A way out of this problem might be the use of continuously melt-replenished Cz growth.

Note that in the literature no difference between B- and Ga-doped Cz-Si has been detected regarding the formation of thermal donors (TDs),[30] clearly indicating that despite the fact that TDs are well known to be oxygen-related complexes, their structure is different from that of the boron-oxygen complex. However, this does not exclude that both kinds of defects are somehow related as will be shown in Sec. VI B.

B. Long-term annealing at low temperature

The defect formation process suggested in this paper is, to a certain extent, similar to the TD formation mechanism proposed by Gösele and Tan.[16] In this mechanism, O_{2i} dimers are captured by other oxygen atoms or clusters to form the higher-order TD levels. In fact, detailed theoretical and experimental work has shown that during the first few hours of TD formation, the concentration of the O_{2i} dimer shows a pronounced decrease.[18,25] As less O_{2i} dimers are available, we expect a decrease in the B_s-O_{2i} concentration and hence a reduced light-induced degradation of the carrier lifetime after

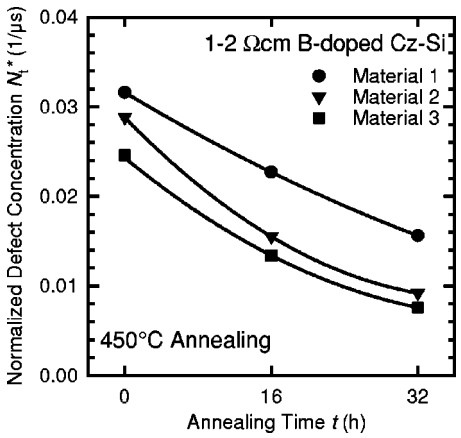

FIG. 10. Reduction in normalized defect concentration N_t^* for three different Cz-Si materials after annealing the samples at 450 °C for up to 32 h.

TD formation. In order to verify our hypothesis, we have annealed different B-doped Cz-Si wafers at 450 °C for up to 32 h.[31] These conditions are ideal for the formation of TDs. As determined from the change in resistivity, after 32 h at 450 °C a TD density of $\sim 5\times10^{15}$ cm^{-3} had been generated in the samples. The evolution of N_t^* as a function of the annealing time is shown in Fig. 10 for three different B-doped Cz-Si materials. After TD formation we measure a pronounced reduction in the metastable defect concentration up to a factor of three. This experimental result is in good agreement with the proposed defect model.

C. Carbon-rich B-doped Cz-Si

Another strategy for reducing the lifetime degradation might be the use of carbon-rich boron-doped Cz-Si. It is well known that the presence of carbon in a high concentration ($>10^{17}$ cm^{-3}) suppresses the TD generation in Cz-Si crystals. This phenomenon has recently been associated with the capture of oxygen dimers by substitutional carbon (C_s).[17] The C_s-O_{2i} formation would be in direct competition with the formation of the lifetime-limiting B_s-O_{2i} complex. Hence, we expect a reduced lifetime degradation in Cz-Si wafers with high carbon content ($>10^{17}$ cm^{-3}). To verify our hypothesis experimentally, we have measured the concentration of the metastable defect in boron-doped Cz-Si wafers with carbon concentrations ranging from $[C_s] = (1.9–3.3)\times10^{17}$ cm^{-3}. Compared to conventional boron-doped Cz-Si, having typical carbon contents below 5×10^{16} cm^{-3}, the concentration of the metastable defect is reduced by about 30% in carbon-contaminated material, making carbon-rich Cz-Si a promising new solar cell material.

VII. CONCLUSIONS

The dependence of the lifetime-limiting metastable defect in boron-doped oxygen-rich silicon on the boron and the oxygen concentrations has been studied. The linear dependence on the boron concentration and the quadratic depen-

dence on the oxygen content indicate the defect to be composed of one substitutional boron and two interstitial oxygen atoms. Formation and annihilation of the metastable boron-oxygen complex have both found to be thermally activated processes, characterized by two strongly differing activation energies of 0.4 and 1.3 eV, respectively. Moreover, the defect generation rate was found to increase proportionally with light intensity below 1 mW/cm^2 and saturate at higher intensities.

Based on these experimental findings, we have developed a defect reaction model to describe the formation and annihilation kinetics of the metastable boron-oxygen-related defect complex. In this model, fast migrating oxygen dimers O_{2i} are captured by immobile substitutional boron B_s to form the lifetime-limiting B_s-O_{2i} complex. The O_{2i} diffusivity is enhanced via a recombination-enhanced diffusion mechanism. Due to the fact that the tetrahedral covalent radius of the B_s atom is 25% smaller than that of the Si host atom, the O_{2i} dimers are preferentially accommodated in the vicinity of a B_s atom. In contrast, the tetrahedral radii of the acceptor atoms Al, Ga, and In are 8–23% *greater* compared to that of the Si atom, hindering the binding of O_{2i} to one of these three acceptors. In good agreement with these considerations, we have not found any lifetime degradation after illumination in Al-, Ga-, and In-doped Cz-Si.

Interestingly, there seems to exist a certain linkage between the B_s-O_{2i} formation and the thermal donor formation in Cz-Si. In the latter process, O_{2i} dimers are believed to be captured by other oxygen atoms or clusters to form the different TD levels. Consequently, the O_{2i} concentration decreases during TD formation. Using lifetime measurements, we have shown that the formation of TDs also leads to a reduced B_s-O_{2i} concentration, indirectly confirming our proposed defect model. The important finding that TD formation and magnitude of light degradation in Cz-Si are directly correlated may open up new possibilities for an effective reduction of the light degradation in Cz-Si solar cells.

ACKNOWLEDGMENTS

The authors thank R. Hezel for his continuous support and encouragement. Funding was provided by the State of Lower Saxony and the German Ministry of Education and Research (BMBF) under Contract No. 01SF0009. The ISFH is a member of the German *Forschungsverbund Sonnenenergie*.

*Email address: j.schmidt@isfh.de

[1] H. Fischer and W. Pschunder, *Proceedings of the 10th IEEE Photovoltaic Specialists Conference*, Palo Alto, CA (IEEE, New York, 1973), p. 404.
[2] J. H. Reiss, R. R. King, and K. W. Mitchell, Appl. Phys. Lett. **68**, 3302 (1996).
[3] J. Schmidt, A. G. Aberle, and R. Hezel, *Proceedings of the 26th IEEE Photovoltaic Specialists Conference*, Anaheim, CA (IEEE, New York, 1997), p. 13.
[4] Y. Ohshita, T. Khanh Vu, and M. Yamaguchi, J. Appl. Phys. **91**, 3741 (2002).
[5] S. W. Glunz, S. Rein, W. Warta, J. Knobloch, and W. Wettling, *Proceedings of the 2nd World Conference on Photovoltaic Solar Energy Conversion*, Vienna, Austria (European Commission, Ispra, 1998), p. 1343.
[6] J. Schmidt and A. Cuevas, J. Appl. Phys. **86**, 3175 (1999).
[7] J. C. Bourgoin, N. de Angelis, and G. Strobl, *Proceedings of the 16th European Photovoltaic Solar Energy Conference*, Glasgow, UK (James & James, London, 2000), p. 1356.
[8] J. Schmidt, K. Bothe, and R. Hezel, *Proceedings of the 29th IEEE Photovoltaic Specialists Conference*, New Orleans, LA (IEEE, New York, 2002), p. 178.
[9] R. A. Sinton and A. Cuevas, Appl. Phys. Lett. **69**, 2510 (1996).
[10] T. Lauinger, J. Schmidt, A. G. Aberle, and R. Hezel, Appl. Phys. Lett. **68**, 1232 (1996).
[11] J. Schmidt, K. Bothe, and R. Hezel, Appl. Phys. Lett. **80**, 4395 (2002).
[12] S. Rein, S. W. Glunz, and G. Willeke, *Proceedings of the 3rd World Conference on Photovoltaic Energy Conversion*, Osaka, Japan, 2003 (in press).
[13] K. Bothe, J. Schmidt, and R. Hezel, *Proceedings of the 3rd World Conference on Photovoltaic Energy Conversion*, Osaka, Japan, 2003 (in press).
[14] H. Hashigami, Y. Itakura, and T. Saitoh, J. Appl. Phys. **93**, 4240 (2003).
[15] S. Rein, T. Rehrl, W. Warta, S. W. Glunz, and G. Willeke, *Proceedings of the 17th European Photovoltaic Solar Energy Conference*, Munich, Germany (WIP, Munich, 2001), p. 1555.
[16] U. Gösele and T. Y. Tan, Appl. Phys. A: Solids Surf. **28**, 79 (1982).
[17] L. I. Murin, T. Hallberg, V. P. Markevich, and J. L. Lindström, Phys. Rev. Lett. **80**, 93 (1998).
[18] Y. J. Lee, J. von Boehm, M. Pesola, and R. M. Nieminen, Phys. Rev. Lett. **86**, 3060 (2001).
[19] F. Shimura, *Semiconductor Silicon Crystal Technology* (Academic Press, San Diego, CA, 1989).
[20] C. P. Ewels, Ph.D. thesis, University of Exeter, UK, 1997.
[21] T. Gregorkiewicz, H. H. P. Th. Bekman, and C. A. J. Ammerlaan, Phys. Rev. B **38**, 3998 (1988).
[22] J. D. Weeks, J. C. Tully, and L. C. Kimerling, Phys. Rev. B **12**, 3286 (1975).
[23] K. Bothe, R. Hezel, and J. Schmidt, Appl. Phys. Lett. **83**, 1125 (2003).
[24] S. W. Glunz, E. Schaeffer, S. Rein, K. Bothe, and J. Schmidt, *Proceedings of the 3rd World Conference on Photovoltaic Energy Conversion* (Ref. 13).
[25] D. Aberg, B. G. Svensson, T. Hallberg, and J. L. Lindström, Phys. Rev. B **58**, 12944 (1998).
[26] J. Schmidt, Appl. Phys. Lett. **82**, 2178 (2003).
[27] T. Saitoh, H. Hashigami, X. Wang, T. Abe, T. Igarashi, S. Glunz, S. Rein, W. Wettling, B. M. Damiani, A. Rohatgi, I. Yamasaki, T. Nunoi, H. Sawai, H. Ohtsuka, T. Warabisako, J. Zhao, M. Green, J. Schmidt, A. Cuevas, A. Metz, and R. Hezel, *Proceedings of the 16th European Photovoltaic Solar Energy Conference* (Ref. 7), p. 1206.

[28] A. Metz, T. Abe, and R. Hezel, *Proceedings of the 16th European Photovolatic Solar Energy Conference* (Ref. 7), p. 1189.
[29] S. W. Glunz, S. Rein, J. Knobloch, W. Wettling, and T. Abe, Prog. Photovoltaics **7**, 463 (1999).
[30] T. Gregorkiewicz, D. A. van Wezep, H. H. P. Th. Bekman, and C. A. J. Ammerlaan, Phys. Rev. B **35**, 3810 (1987).
[31] K. Bothe, J. Schmidt, and R. Hezel, *Proceedings of the 29th IEEE Photovoltaic Specialists Conference* (Ref. 8), p. 194.